

MODIFIED CLAD OPTICAL FIBRE COATED WITH PVA/TiO₂ NANO COMPOSITE FOR HUMIDITY SENSING APPLICATION

Chandra Khatua^a, Ipsita Chinya^a, Debdulal Saha^b, Shyamal Das^a, Ranjan Sen^a and Anirban Dhar^{a*}

^aAcademy of Scientific and Innovative Research, Fibre Optics and Photonics Division, CSIR-Central Glass & Ceramic Research Institute

^bSensor and Actuator Division, CSIR-Central Glass and Ceramic Research Institute
196, Raja. S. C. Mullick Road, Kolkata-700 032, India

*Email: anirband@cgcricri.res.in

Submitted: May 3, 2015

Accepted: July 29, 2015

Published: Sep. 1, 2015

Abstract- Synthesis of TiO₂ nanoparticle through hydrolysis method is presented followed by TiO₂-nanoparticle doped polyvinyl alcohol nanocomposite by solution process. FTIR, XRD, DSC-TGA, FESEM, TEM analysis are used to identify the nature of synthesized nanoparticle and loading uniformity of developed composite material. A simple modified clad based optical fibre sensor is developed to measure relative humidity. Coated modified clad optical fibre exhibits excellent relative humidity sensing performance with improved thermal stability of coating material in wide range of 9-95 % RH with good process repeatability. Sensor response is also observed to be very fast and highly reversible. Advantage of our developed composite material become evident when it exhibits wider range of moisture sensitivity compare to pure PVA or pure TiO₂ material found in literature. Performance of PVA-TiO₂ nanocomposite thick film is also evaluated by capacitance method and result found to agree with coated modified clad optical fibre.

Index terms: Polyvinyl alcohol, titanium dioxide, nanocomposite, modified-clad optical fibre, relative humidity sensor.

I. INTRODUCTION

Humidity is a physical quantity that has significant importance in many medical and industrial applications namely in the diagnosis of pulmonary diseases [1], for mapping the human respiratory system [2] by monitoring the water vapor content of exhaled breath, meteorological applications to predict likelihood of precipitation, dew or fog, in incubators, pharmaceutical processing, textile production, building automation etc. Accordingly, controlling, sensing and monitoring of humidity are presently gaining a lot of research interest [3]. There are different traditional electrical humidity sensors available which have been exploited to measure relative humidity (RH) for the above mentioned application based on resistive, capacitive and hygrometric ones [4]. However, these conventional electrical methods for sensing RH, is associated with several drawbacks such as their high cost, regular maintenance, inability to be employed in hazardous or explosive environments and interaction with electromagnetic signals.

Research and studies on polymeric humidity sensors have continued and used in the industry over the past decades. Most of these sensors are fabricated based on thin films of porous polymers, and the sensing principles are similar to that of metal oxide ceramic sensors [5]. The functionality of the sensor is based on the physical and chemical absorption of moisture by the films and condensation of moisture in the pores, and therefore a change in some physical and electrical properties of the transducer. However, the demand for organic polymer based humidity sensors and its applications still have a lower degree of satisfaction compared with that for ceramic metal-oxide thick or thin film sensors although their fabrication and development has improved gradually to enhance their practical pertinence. However, optical fibre coated with thin polymeric film can provide cutting edge due to their high sensitivity, resistance towards electromagnetic interference, corrosion resistance, easy construction of large sensor network and remote sensing network ability. RH sensors based on fibre-optic techniques, can be classified according to the methods on which they rely, namely direct spectroscopy [6], fibre bragg gratings [7], interferometry [8] and evanescent wave based [9]. These mentioned techniques have their own advantages and disadvantages out of which FBGs based humidity sensor offers a wide response range, but it is easily disturbed by temperature, strain etc. and needs expensive and complex technology. Accordingly, research is continuing to develop improved materials with better and enhanced technique for RH sensing which can be cheap and easy to implement in practical application. The fibre-optic sensor using cladding modification methodology is very interesting because of its wide

dynamic range, high sensitivity, easy to fabricate and can be constructed by simple optical design for remote sensing [10-12].

Polyvinyl alcohol (PVA) is already implemented for humidity sensors [13, 14] while TiO_2 with nano sized powders [15] are potential candidate for gas sensing [16], photo-catalysts, photo-electrodes for photo-splitting water, and solar energy conversion etc. [17]. Among the different phases of titanium dioxide, anatase phase is widely accepted for sensing applications[18]. Based on this background, here we report synthesis and characterization of a polymer composite based on PVA doped with TiO_2 nanoparticle [19-22]. The humidity sensing performance of this composite material over modified clad optical fibre is also evaluated and found to exhibit excellent performance in the range of 9 to 95% RH. Finally, the performance of the same material as a thick film under controlled atmosphere condition is also measured by capacitance method under controlled atmosphere and result established that our developed materials is a potential candidate for humidity sensing application covering a wide RH range with good process repeatability.

II. EXPERIMENTAL

a. Experimental set-up:

The performance of the sensor was tested by placing the sensor in a humidity chamber with a volume of 5 liter held at 25°C within a thermostatic housing. The desired humidity level was controlled by using different kind of chemical salt solution which was optimized for a particular % of relative humidity. The environment in the chamber was monitored by SHAW Dew point meter & Relative Humidity meter (Fig.1).

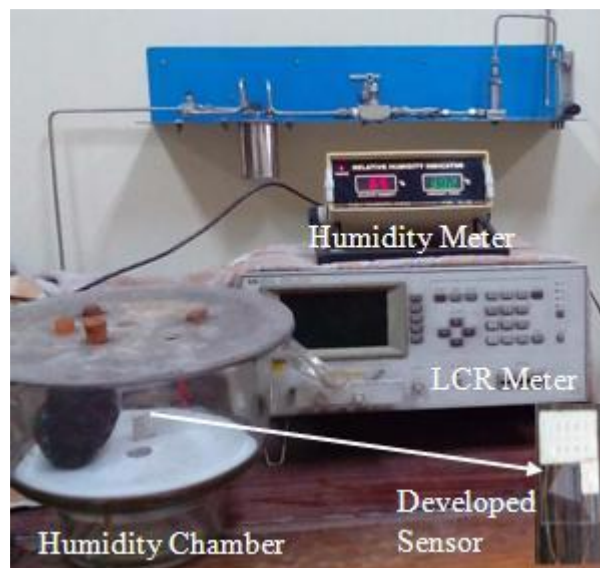


Figure.1 Sensor testing set-up

b. Synthesis and characterization of TiO₂ nanoparticles

Titanium dioxide nanoparticles were synthesized using hydrolysis of titanium tetrachloride (Loba Chemie, Mumbai, India) as the starting material in presence of urea (Merck) solution under constant stirring at 150°C [23]. The homogeneous solution obtained was allowed to settle down and separated by centrifugation followed by washing with water ethanol solution several times. The precipitate was then dried in an oven at 120°C, ground to fine powder using agate mortar followed by calcinations at different temperatures (400°C, 600°C, 700°C, 800°C and 1000°C) for 4 h.

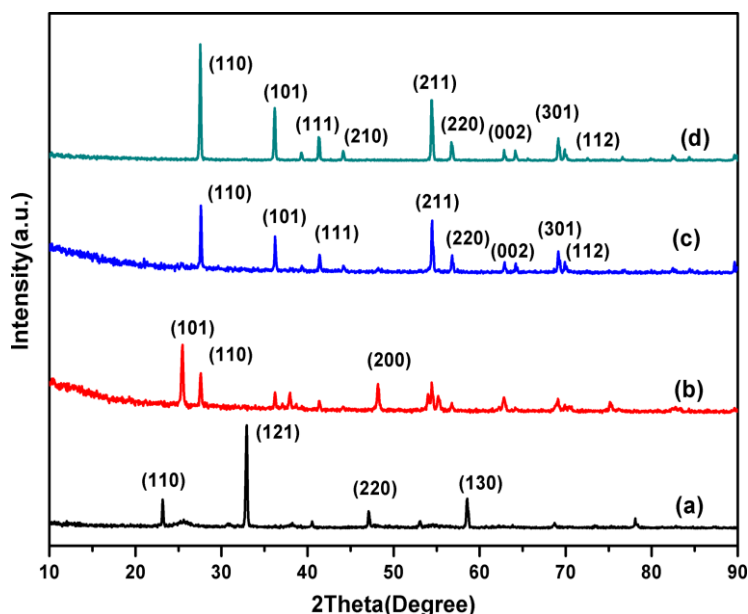


Figure.2 XRD pattern of titanium dioxide synthesized and calcined at different temperature
(a) synthesized, (b) 700°C, (c) 800°C, and (d) 1000°C

X-ray diffraction (XRD) (PANalytical, X'Pert Pro MPD, The Netherlands) studies of synthesized particle calcined at different temperatures is presented in Fig. 2. The diffraction patterns of as synthesized powder is well indexed to the rhombohedral structure (JCPDS No. 85-0868), calcination at 700 °C transforms this into anatase phase of TiO₂ (JCPDS no. 84-1286), and calcination at 800 °C and 1000°C transforms into rutile phase of TiO₂ (JCPDS no. 86-0147). Diffraction peaks corresponding to the impurity are not found in the XRD patterns, confirming high purity of synthesized sample. The increase in intensity of the XRD peaks with calcinations temperature indicates increased crystallinity while crystallite size for derived particle is calculated using Debye-Scherrer's formula as presented in Table 1.

Table1: Crystallite size of titanium dioxide at different calcination temperature

Sample	Crystallite Size(nm)
As Synthesized TiO ₂	32
Calcined powder at 400° C	8
Calcined powder at 600° C	17
Calcined powder at 700° C	34
Calcined powder at 800° C	41
Calcined powder at 1000° C	50

In Fig. 3 fourier transform infrared spectroscopy (FTIR) of TiO₂ exhibits peaks at 3140cm⁻¹ and 1660 cm⁻¹ due to the stretching and bending vibration of the -OH group while the peak at 580 cm⁻¹ shows stretching vibration of Ti-O and peaks at 1400 cm⁻¹ shows stretching vibrations of Ti-O-Ti [24].

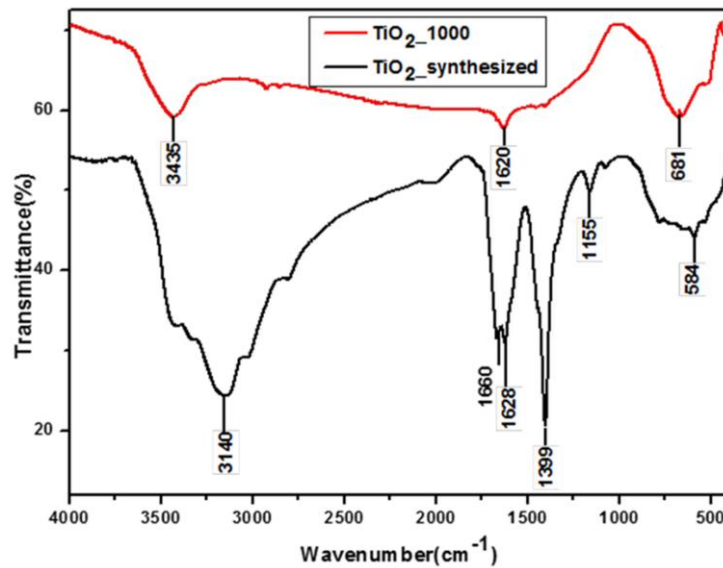


Figure.3 FTIR spectra for titanium dioxide synthesized and calcined at 1000° C

The comparison of field emission scanning electron microscopic pictures (FESEM) of synthesized titanium dioxide with that of calcinated samples are presented in Fig. 4 clearly indicates that synthesized TiO₂ particles exhibit irregular morphology due to the

agglomeration of primary particles but spherical morphology achieve after calcination process. EDX analysis also confirms the presence of Ti without any impurity after calcination.

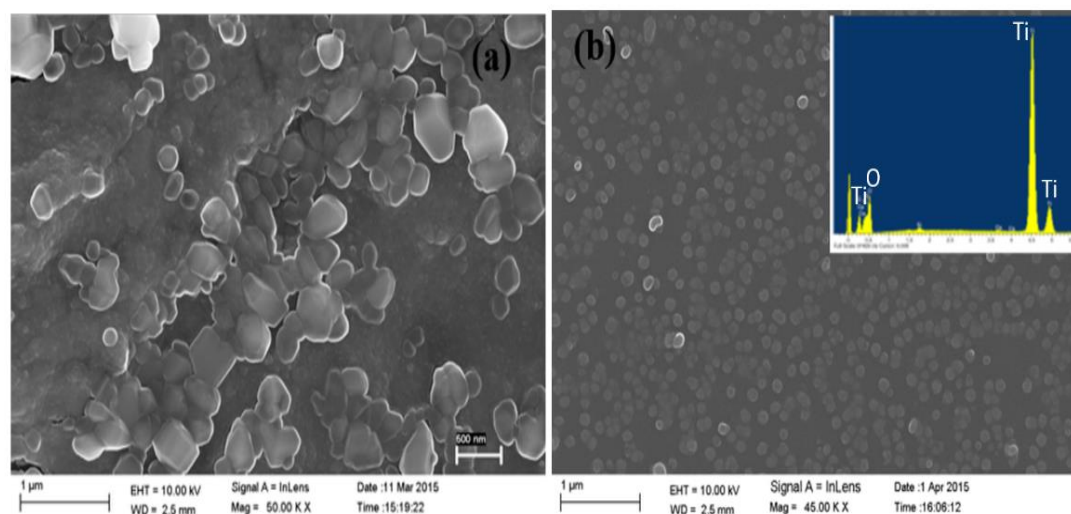


Figure. 4 FESEM micrograph of (a) synthesized and (b) calcined titanium dioxide along with EDX analysis (inset of Fig. 4 b)

The structural and chemical natures of synthesized particles are further investigated using high resolution transmission electron microscopy (HRTEM) and associated energy dispersive x-ray spectroscopy (EDX). TEM samples were prepared by dispersing the powder in ethanol by ultrasonic treatment, dropping onto a porous carbon film supported on a copper grid, and then drying in air. All TEM images and diffraction patterns are taken with 200 keV. Bright field TEM image of the calcined powder is presented in Fig. 5a. Analysis of SAED pattern confirms that, synthesized samples are relatively polycrystalline containing nano crystals as presented in Fig. 5b. HRTEM image is shown in Fig. 5c. High resolution TEM image (Fig 5c) also confirmed that during the heat treatment of the synthesized powder, crystallization is achieved which exhibited lattice fringes corresponding to d -spacing of 0.317nm which is consistent with the spacing of most predominant (110) planes of the primitive tetragonal TiO₂ crystal. The EDX spectra presented in Fig. 4d confirms the chemical composition of sample containing Ti and O only with Ti: O ratio of 1:2.

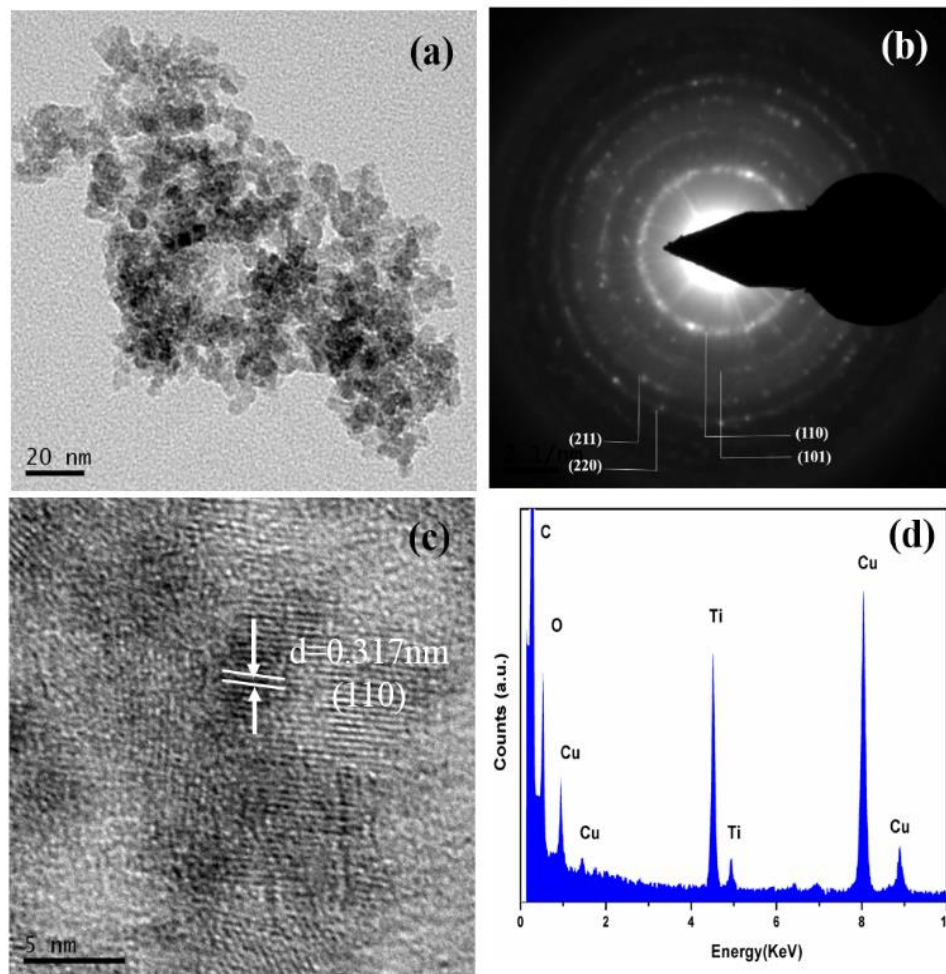


Figure.5 TEM image of the calcined powder of TiO_2 (a) bright field image of the powder, (b) SAED image of the powder, (c) HRTEM image of the powder, (d) EDX of powder

Differential scanning calorimetric and Thermo gravimetric analysis (DSC-TGA) of synthesized samples are presented in Fig. 6. TGA curves of our sample reveals two main weight loss regions associated with water loss. From DSC, the first region at a temperature of 98°C is due to the evaporation of physically weakly and chemically strongly bounded water. From DSC curve the peak at around 738°C indicates the phase transformation of TiO_2 from anatase to rutile.

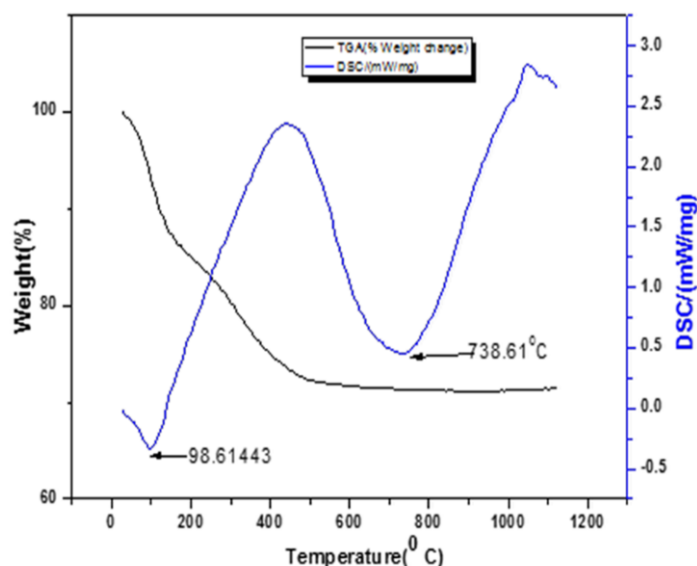


Figure.6 DSC and TGA curve of synthesized titanium dioxide material

c. Synthesis and characterization of polymer composite

The PVA (Loba Chemie) solution was prepared by dissolving requisite amount of PVA powder in de-ionized (DI) water with vigorous stirring at 60° C for 1 h, followed by addition of requisite amount of synthesized TiO₂ nanoparticle at 40°C. Stirring was continued until a homogeneous solution was obtained. The weight percentage of PVA solution was varied from 3-15% while TiO₂ loading level varied from 0.5-5 weight % in order to achieve the polymer composite for different experiments and optimization process. The schematic of preparation process is given in Fig. 7. The selection of TiO₂ has manifold advantages namely increased amorphous nature of PVA film, better thermal stability and improved moisture sensitivity.

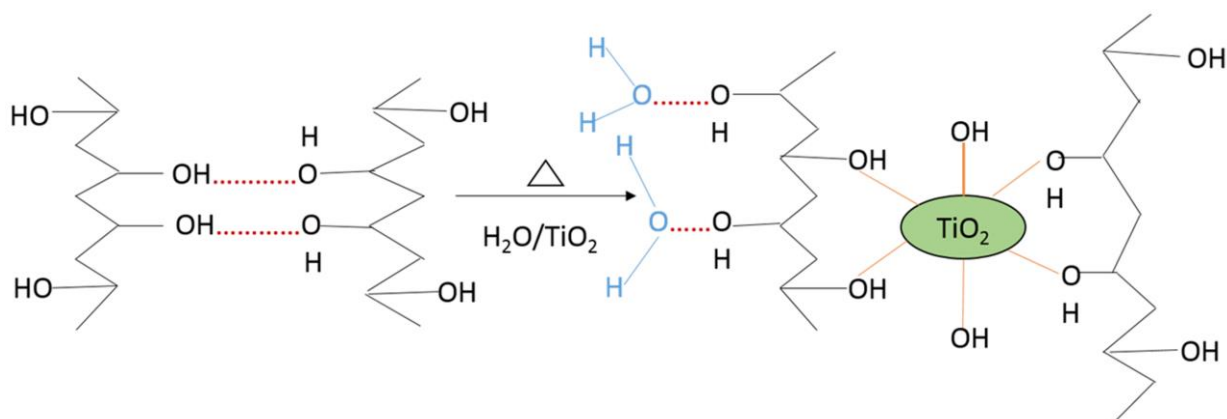


Figure.7 Schematic of PVA-TiO₂ composite during synthesis

The comparison of XRD pattern (Fig.8) in the range of 15 to 60° of the pure PVA film with that of PVA-TiO₂ composite clearly reveals that, the addition of TiO₂ in polymer reduces the intensity of the main PVA peak followed by a broadening of the peak area leading to increase in the degree of amorphousity. Additionally the separate peaks indicate the presence of TiO₂.

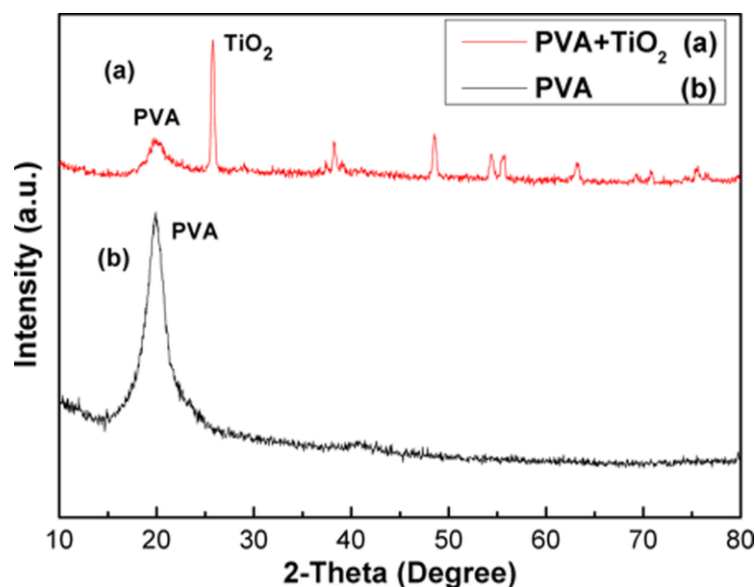


Figure.8 XRD pattern of PVA and PVA-TiO₂ composite film

TGA curves of PVA and PVA/TiO₂ composite is compared in Fig. 9 which exhibited that the decomposition temperature for PVA-TiO₂ about 60°C higher compared to pure PVA. This undoubtedly established better thermal stability of the polymer composite as a result of homogeneous loading of TiO₂ into PVA matrix. This increase in thermal stability originates as a result of strong interactions between TiO₂ particles and polymer matrix. The interaction between TiO₂ and PVA chains restricts the thermal motion of macromolecules which enhances the rigidity of macromolecular chain and more energy needs for movement of polymeric chain.

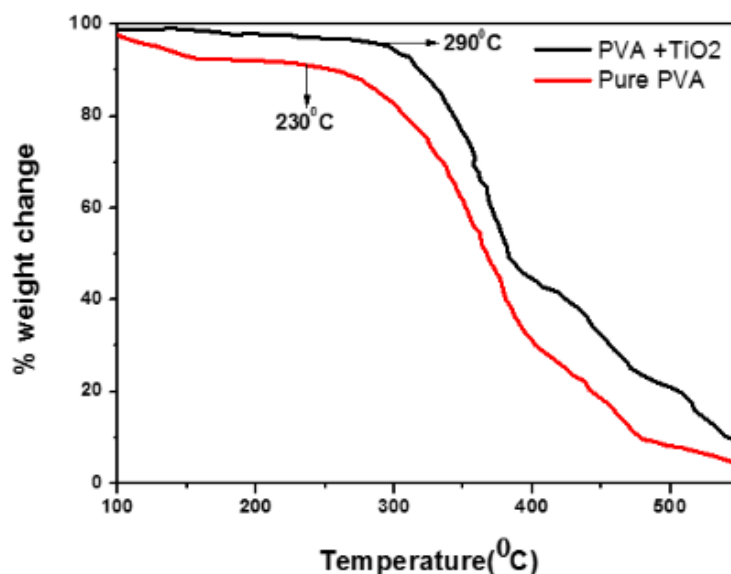


Figure.9 TGA analysis of PVA and PVA-TiO₂ composite film

Comparison of FESEM images of PVA and developed polymer composite reveals that doped TiO₂ is homogeneously distributed throughout the PVA membrane as evident from Fig. 10a. The white particle visible in Fig. 10a is due to high atomic weight of Ti which has been confirmed from spot EDX analysis of the sample. The cross sectional view in Fig. 10b of the same film reveals that the surface structure comprised of large pores along with many nano pores leading to enhancement of the active surface area which is responsible for the high absorption ability of the developed material. The uniform dispersion and pore size are found to be influence substantially by PVA wt % during preparation of polymer composite.

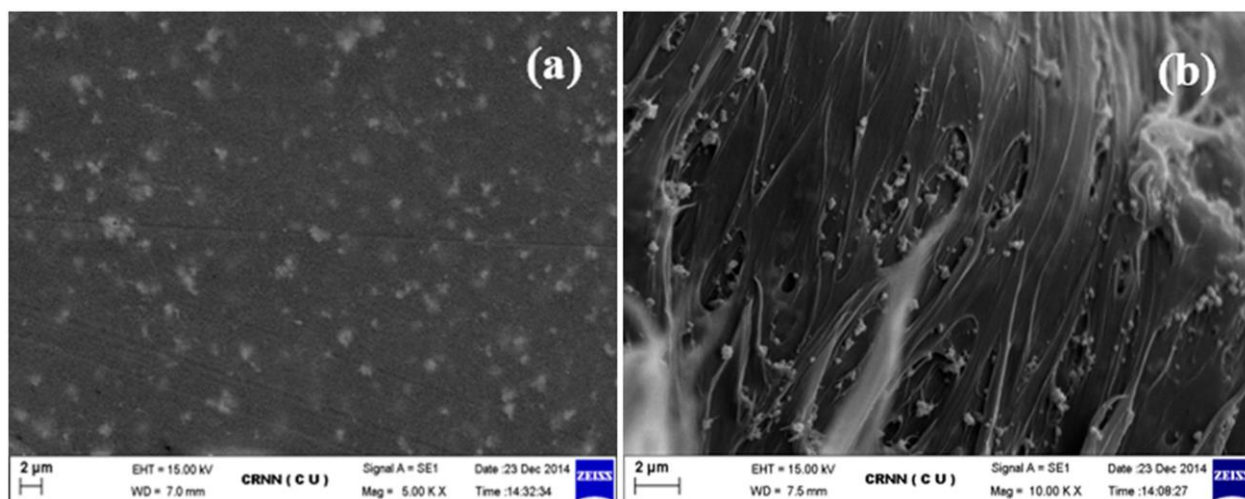


Figure.10 FESEM micrograph (a) PVA-TiO₂ composite film, (b) Cross sectional view of PVA- TiO₂ composite film

FTIR spectra of pure PVA and developed composite films are presented in Fig.11. The spectra consists of a strong broad band at 3435 cm^{-1} corresponds to OH stretching vibration of hydroxyl groups of PVA. The band corresponding to C-H asymmetric stretching vibration occurred at 2928 cm^{-1} and C-H symmetric stretching vibration is observed at 2859 cm^{-1} . The observed bands at 1635 cm^{-1} correspond to C-C group and can be explained on the basis of intra/inter molecular hydrogen bonding with the adjacent O-H group. A band at 1093 cm^{-1} corresponds to C-O stretching of acetyl group present in the PVA back bone. The corresponding bending, wagging of CH_2 vibrations is observed at 1468 cm^{-1} . For PVA and TiO_2 composite, the peak at 467 cm^{-1} show stretching vibration of Ti-O.

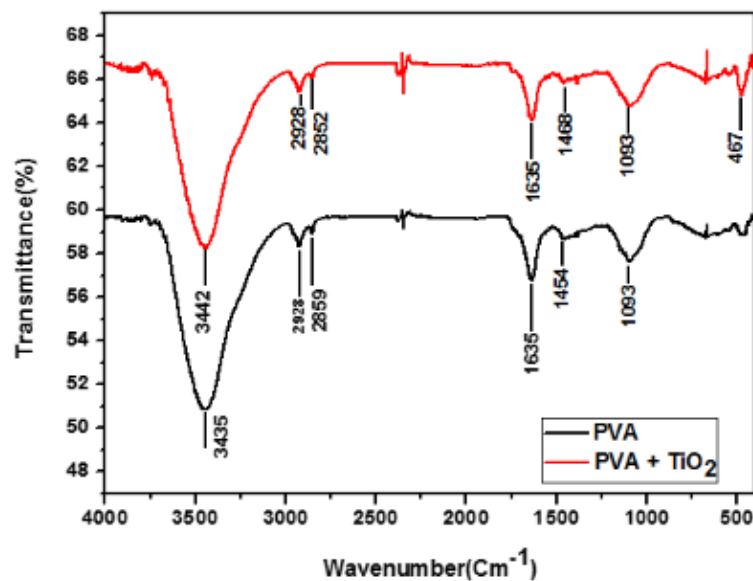


Figure.11 FTIR spectra of pure PVA and PVA TiO_2 composite film

d. Fabrication and sensing experiment with PVA- TiO_2 coated modified clad optical fibre

A standard single mode fibre (SMF) with core diameter $8\mu\text{m}$ w.r.t $125\mu\text{m}$ cladding diameter was etched using optimized etching solution for stipulated time period after removing out the polymer jacket. The etched fibre diameter was varied from 30 to $8\mu\text{m}$ in different experiments to optimize the sensing performance. This modified-clad optical fibre sample was then coated with developed polymer composite using dip-coating machine (Delta Scientific, India) maintaining optimized dipping speed to achieve desired coating thickness and coating uniformity followed by curing at 80°C under an inert gas atmosphere. Coating thickness of the modified-clad optical fibre was varied from 10 to $50\mu\text{m}$. The optimised coating thickness (Fig.12) of the modified clad optical fibre was taken in this experiment.

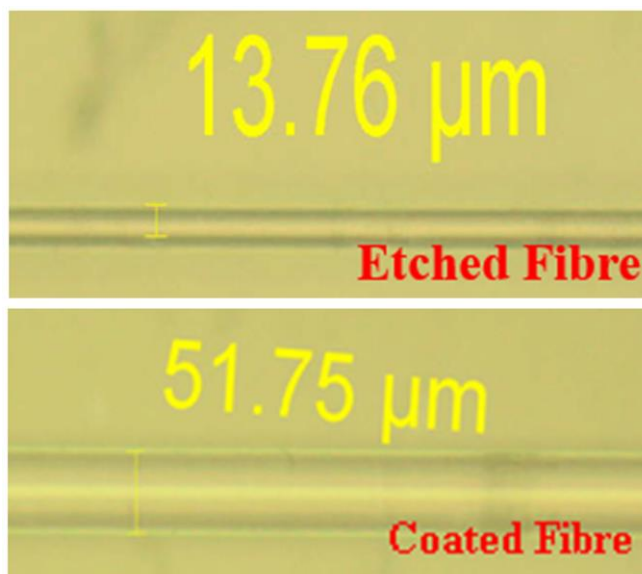


Figure.12 Image of etched and coated fibre

A small length (~ 5 cm) of the modified clad optical fibre coated with thin layer of PVA-TiO₂ composite then spliced with SMF at two ends and its absorption in the wavelength range of 400-1700 nm was recorded using Bentham Set-up (UK). The schematic of experimental set-up is given in Fig. 13.

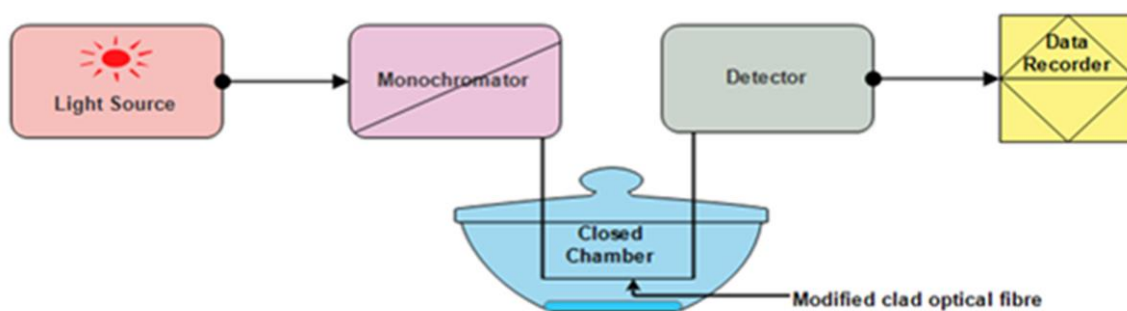


Figure.13 Schematic of experimental set up for sensing experiment

The relative humidity (RH) characteristics of sensing polymeric material coated modified clad optical fibre were investigated by exposing them sequentially to a range of different humidity conditions at a constant room temperature. Five different types of chemical salt solutions were used in this work to create RH conditions at 9, 25, 48, 72, 83, and 95% RH. This method provides a simple yet effective means of RH calibration, which is relatively easy and convenient to set-up in laboratory. The test chamber capacity and solution surface area-to-chamber volume ratio were taken into consideration.

In order to evaluate repeatability of the sensing performance, the coated fibre sample was dried after each sensing experiment around 100°C for 30 minutes to ensure evaporation of any absorbed moisture in the coating layer followed by repeating sensing performance again. This repeatability experiment was performed up to 3 cycles.

III. RESULT & DISCUSSION

This sensing performance is based on the phenomenon of evanescent wave absorption where a small portion of the optical power in the guided modes, extended to the cladding region, interacts with the coated sensing polymeric composite material. Water molecule has a strong absorption around 1380 nm. The results obtained are plotted in Fig. 14a. Fig. 14a reveals that there is a significant change in transmission peak at 1380nm with variation of % RH. The reason behind the change in transmission spectra with moisture level is due to affinity of PVA-TiO₂ composite material towards moisture. Due to absorption and desorption of water molecule the refractive index changes with change in moisture level. This change in refractive index then alters the intensity of transmission peak around 1380 nm as evident from Fig. 14a. From chemical view point, when PVA-TiO₂ coating material is exposed to water it swells due to formation of weak secondary bonding with the OH-group present in PVA; the swelling of the coating layer changes with change in moisture level and results in variation of layer density of composite coating material which in turn changes the refractive index of the coating layer. From graph 14b the RH response of the sensors is found to be linear with increasing RH from 9 to 95 % RH. This result clearly shows that our developed composite material exhibit better sensitivity performance compared to pure PVA (50 to 90%) [25-26] and pure TiO₂ (10 to 62%) RH range [16], [27]. A long period grating humidity sensor coated poly(ethylene oxide)/CoCl₂ can detect RH variation in the range from 50% to 95% [28]. Response time of the optical fibre humidity sensor based on nanocoatings applying the electrostatic self-assembly technique is lesser than 300 ms, but the dynamic sensing range is 75–100% RH [29]. A tapered optical fibre based humidity sensor using nanostructured sensitive coating shows changes in RH from 75% to 100% [30]. For SiO₂ nanoparticle coated optical fibre based humidity sensor maximum sensitivities have been achieved at a high humidity range of 83.8%RH to 95.2%RH [31].

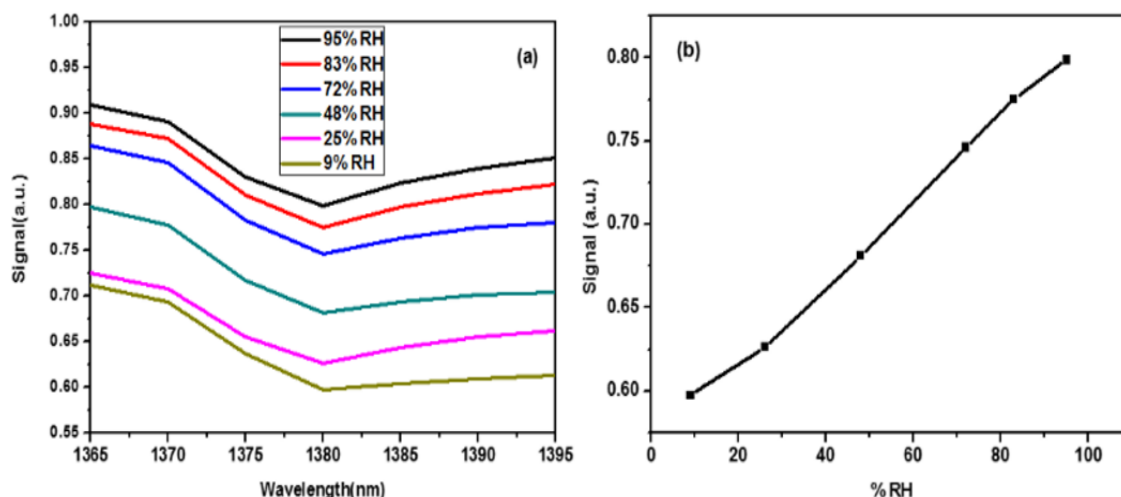


Figure.14 (a) Intensity modulation of signal with varying %RH at 1380 nm, (b) Transmission signal change with varying %RH at 1380nm

The time response characteristic of the humidity sensor depends on a number of factors including the diffusion rate of the water molecules in the coated polymer composite, the rate of swelling and the thickness of the coated sensing material. In this study, the time response characteristics of sensors with different % RH are investigated at a constant temperature of 23°C. The airtight enclosures of similar capacities are pre-saturated at different % RH using different chemical salt solutions. Sufficient time gap was maintained to achieve equilibrium at different % of RH solution to acquire stable experimental data. The recovery time of the sensors which is defined as time to recover original signal, is also investigated and recovery curves of the sensors are plotted in Fig. 15a. Fig.15a exhibited that depending on the exposure time, the transmittance signal becomes constant after 30 s after which no further change in intensity is observed. Response time of the sensor which is defined as time of 90% change in signal, is 27s. A possible explanation could be complete saturation of the coated polymeric layer by diffused water molecules.

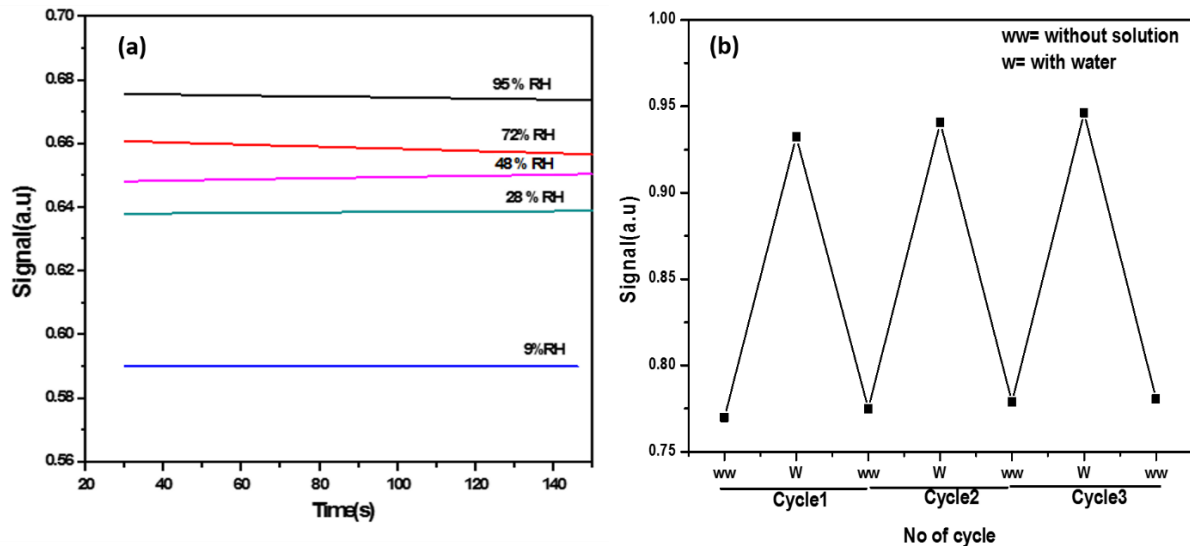


Figure.15 (a) Plot of Transmittance signal at 1380nm various humidifies against the soaking time variation, (b) Repeatability plot of modified clad fibre in presence and absence of water

The repeatability performance of the fibre sample is found to be acceptable even after 3 cycles as presented in Fig.15b which indicates that our developed composite materials exhibited good process repeatability besides liner performance in the range of 9 to 95 % RH.

a. Preparation and sensing experiment with PVA-TiO₂ thick film using capacitance method

It is beyond our limit to control % RH in closed chamber in laboratory during testing of modified clad optical fibre sensor. Accordingly, we utilized capacitive method by which the % RH sensitivity of the same sensing polymeric composite material could be evaluated in closed chamber in a control manner [32-33]. The PVA-TiO₂ composite thick film was prepared using conventional solution method over a glass substrate which contains coating of a conductive paste of silver composite. Another layer of conductive paste was deposited over the PVA-TiO₂ film to form parallel electrode. The film thickness was varied in different experiment within 0.25-0.28 mm by capacitance method. The electrical performance of the sensor was then examined by placing the samples in a chamber with a volume of 250 cc held at 25°C within a thermostatic housing. The desired humidity level was controlled by using different kind of chemical solution which was optimized for a particular % of relative humidity. The environment in the chamber was monitored by SHAW Dew point meter (model no. SADPTR-R). The schematic of the actual experimental set-up is presented in Fig. 16 while actual system is presented in Fig. 1.

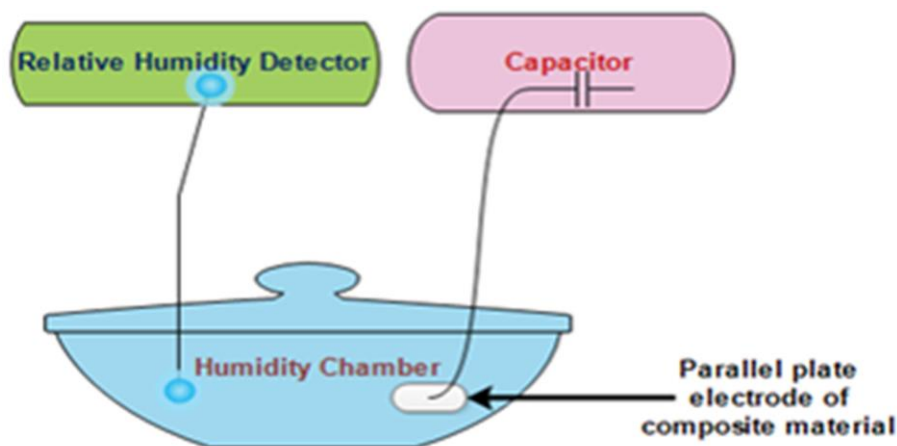


Figure.16 Schematic of experiment set up for sensing measurement for polymer composite film

It is observed that change in % RH of the solution capacitance changes at constant frequency (1 kHz) as presented in Fig. 17. The result clearly indicates that at lower humidity range change of capacitance with % RH is less whereas at higher %RH the change of capacitance is sharp. Variation of dielectric constant occurred due to different level of moisture absorbed by pores of composite material according to moisture content in the closed atmosphere. The water molecule has six degrees of freedom. When the water molecule enters the pores it loses its degree of freedom and a change of state would take place from moisture vapor to liquid and overall dielectric constant of the material will be increased. At low % RH range less water molecules enter into the pores leading to small change in capacitance while at higher % RH range water molecules tend to form cluster into the pores of polymeric composite material and therefore sharp change of capacitance occurs at higher % RH range. Fig. 17 also exhibits a comparison of PVA-TiO₂ nanocomposite material with polymeric composite material consisting PVA-TiO₂ micro particle and pure PVA, which establishes that our synthesized PVA-doped with TiO₂ nanoparticle exhibits excellent performance and is a potential candidate for humidity sensing purpose within the range of 9 to 95% RH. PVA and TiO₂ nanocomposite shows better performance than pure PVA and PVA micro particle.

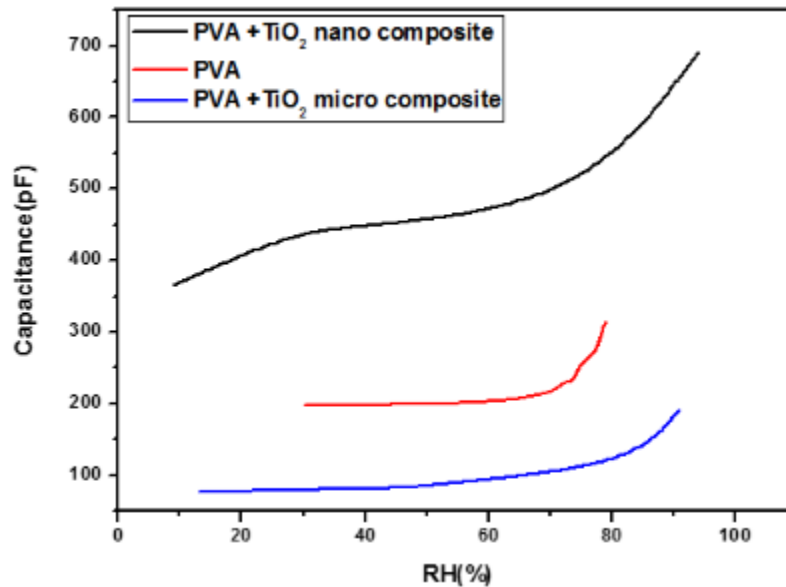


Figure.17 Capacitance of polyvinyl alcohol and titanium dioxide composite film using titanium dioxide nano and micro particle as humidity sensor

IV. CONCLUSION

We present synthesis and characterization of PVA loaded TiO₂ nanoparticle polymeric composite material. The performance of developed polymer composite towards humidity sensing is also evaluated by coating them over modified clad optical fibre which exhibited good moisture sensing performance with excellent process repeatability and response time of 27s and recovery time of 30s. The measurement is insensitive to temperature. It also has advantages of robustness, low cost, and easy operation in practical applications. Additionally, we report experimental result of PVA-TiO₂ composite thick film's moisture sensitivity performance using capacitance method and the sensitivity graph (Fig.16) exhibited quasi-linear change with capacitance over 9-95% RH range and established that our developed material is a potential candidate for fibre optic humidity sensor.

V. ACKNOWLEDGEMENT

Authors acknowledge the financial support of CSIR, India and two authors C. Khatua and I. China thankfully acknowledge AcSIR-CSIR (CGCRI) for providing academic support.

REFERENCES

- [1] C. Laville, "Pellet Interdigitated humidity sensors for a portable clinical microsystem", *IEEE Trans Biomed Eng*, vol.49, no.10, 2002, pp. 1162–1167.
- [2] A. H. M. Habib Ahsan, C. F. Lange, W. Moussa , "Development of a Humidity Microsensor with Thermal Reset", In *Proceedings of the International Conference on MEMS, NANO and Smart Systems*, Banff, AB, Canada, 20–23 July, 2003, pp.89-93.
- [3] S. A. Kolpakov, N. T. Gordon, C. Mou, K. Zhou, "Toward a new generation of photonic humidity sensors" *Sensors*, vol.14 , no.3, 2014, pp. 3986-4013.
- [4] S. F. H. Correia, P. Antunes, E. Pecoraro, P. P. Lima , H. Varum , L. D. Carlos, R.A.S. Ferreira , P.S. Andre, "Optical Fibre Relative humidity sensors based on a FBG with a Di-Ureasil coating" *Sensors*, vol.12, no.7, 2012 , pp. 8847-8860.
- [5] D. K. Ghara, D. Saha and K. Sengupta, "Leak rate and location analysis through slits and cracks in pipes by nano porous ceramic humidity sensors", *International journal on smart sensing and intelligent systems*, vol. 1, no. 3, september 2008, pp.784-798
- [6] M. Bedoya, M. T. Diez, M. C. Moreno-Bondi, G. Orellana, "Humidity sensing with a luminescent Ru(II) complex and phase-sensitive detection" *Sens Actuators B Chem* vol. 113, no.2, 2006, pp.573–581.
- [7] M. Konstantaki, S. Pissadakis, S. Pispas, N. Madamopoulos, and N.A. Vainos, "Optical fibre long-period grating humidity sensor with poly (ethylene oxide)/cobalt chloride coating" *Appl Opt*, vol. 45, no.19, 2006, pp.4567–4571.
- [8] T. Venugopalan, T. L.Yeo,T. Sun, and K.T.V. Grattan "LPG based PVA coated sensor for relative humidity measurement", *IEEE Sens J*, vol. 8, no.7, 2008, pp. 1093–1098.
- [9] J.M. Corres,J. Bravo, I.R. Matias,F. J. Arregui, "Nonadiabatic tapered single-mode fibre coated with humidity sensitive nanofilms" *IEEE Photon Technol Lett*, vol. 18, no.8, 2006, pp. 935–937.
- [10] M.A. El-Sherif, "On-Fibre sensor and modulator" *IEEE Trans Instrum Meas* vol.38, no.2, 1989, pp. 595–598.
- [11] M. A. El-Sherif, "An Apparatus and a Method Comprising an Optical Fibre Modulator, Coupler, Switch, Sensor, and Distribution System (1991) U.S. Patent 5 060 307.
- [12] P. J. Rivero, A. Urrutia, J. Goicoechea, F. J. Arregui, I. R. Matías, "Humidity sensor based on silver nanoparticles embedded in a polymeric coating", *International journal on smart sensing and intelligent systems*, vol. 5, no. 1, march 2012, pp.71-83.
- [13] J. An, Y.Zhao, Y. Ji,C. Shen, "Relative humidity sensor based on SMS fibre structure with polyvinyl alcohol coating" , *Optik- International journal for light and electron optics*, vol. 124, no.23, 2013, pp. 6178-6181.
- [14] X. Dong, T. Li, Y. Liu, Y. Li, C. L. Zhao,C.C. Chan " Polyvinyl alcohol–coated hybrid fibre grating for relative humidity sensing" , *J Biomed Opt*, vol. 16, no.7, 2011, pp. 077001.
- [15] K. Thangavelu,R. Annamalai ,D. Arulnandhi, "Preparation and Characterization of Nanosized TiO₂ Powder by Sol-Gel Precipitation Route" *Int J Emerg Technol Adv Eng*, vol. 3, no.1, 2013,pp.636-639.
- [16] S.K. Shukla, A. Bharadvaja, G.K. Parashar, A.P. Mishra, G.C. Dubey,A.Tiwari , "Fabrication of ultra-sensitive optical fibre based humidity sensor using TiO₂ thin film" *Adv Mat Lett* ,vol 3, no.5, 2012,pp. 365-370.

- [17] D. V. Bavykin, J. M. Friedrich, F. C. Walsh, "Protonated titanates and TiO₂ nanostructured materials: synthesis, properties, and applications", *Adv Mater*, vol. 18, no. 21, 2006, pp. 2807–2824.
- [18] Z. Chen Z, C. Lu, "Humidity Sensors: A Review of Materials and Mechanisms" *Sensor Letters*, vol. 3, 2005, pp. 274–295.
- [19] J. Ahmad, K. Deshmukh, M. Habib, M. B. Hägg, "Influence of TiO₂ Nanoparticles on the Morphological, Thermal and Solution Properties of PVA/TiO₂ Nanocomposite Membranes", *Arab J Sci Eng*, vol. 39, no. 10, 2014, pp. 6805–6814.
- [20] R. Singh, S. G. Kulkarni, S. S. Channe, "Thermal and mechanical properties of nano titanium dioxide-doped polyvinyl alcohol", *Polym Bull*, vol. 70, no. 4, 2013, pp. 1251–1264.
- [21] A. Maurya, P. Chauhan, "Synthesis and characterization of sol–gel derived PVA-titanium dioxide (TiO₂) nanocomposite", *Polym Bull*, vol. 68, no. 4, 2012, pp. 961–972.
- [22] P. Ahmadpoor, A. S. Nateri, V. Motaghitalab, "The optical properties of PVA/TiO₂ composite nanofibres", *J Appl Polym Sci*, vol. 130, no. 1, 2012, pp. 78–85.
- [23] V. Parthasarathi and G. Thilagavathi, "Synthesis and Characterization and Their Application to Textile for Microbe Resistance," *Journal of Textile Apparel Technology and Management*, Vol. 6, No. 2, 2009, pp. 1–8.
- [24] H. Pana, X. D. Wang, X. X. Xiao, L. G. Yu, Z. J. Zhang, "Preparation and characterization of TiO₂ nanoparticles surface-modified by octadecyltrimethoxysilane", *Indian J Eng Mater S*, vol. 20, 2013, pp. 561–567.
- [25] W. C. Wong, C. C. Chana, L. H. Chena, T. Li, K. X. Leea, K. C. Leong, "Polyvinyl alcohol coated photonic crystal optical Fibre sensor for humidity measurement", *Sensors and Actuat B-Chem*, vol. 174, 2012, pp. 563–569.
- [26] A. Gaston, I. Lozano, F. Perez, F. Auza, J. Sevilla, "Evanescent wave optical-fibre sensing (temperature, relative humidity, and pH sensors)", *IEEE Sens J*, vol. 3, no. 6, 2003, pp. 806–811.
- [27] T. Islam, Z. U. Rahman and S. C. Mukhopadhyay, "A Novel Sol–Gel Thin-Film Constant Phase Sensor for High Humidity Measurement in the Range of 50%–100% RH", *IEEE Sensors Journal*, Vol. 15, No. 4, April 2015, pp. 2070–2076.
- [28] A. A. Herrero, H. Guerrero, D. Levy, "High-sensitivity sensor of low relative humidity based on overlay on side-polished fibres", *IEEE Sens J*, vol. 4, no. 1, 2004, pp. 52–56.
- [29] M. Konstantaki, S. Pissadakis, S. Pispas, N. Madamopoulos, N. A. Vainos, "Optical fibre long-period grating humidity sensor with poly (ethyleneoxide)/cobalt chloride coating", *Appl Opt*, vol. 45, no. 19, 2006, pp. 4567–4571.
- [30] I. R. Matias, F. J. Arregui, J. M. Corres, J. Bravo, "Evanescent field fibre-optic sensors for humidity monitoring based on nanocoatings" *IEEE Sens J*, vol. 7, no. 1, 2007, pp. 89–95.
- [31] J. M. Corres, F. J. Arregui FJ, I. R. Matias, "Sensitivity optimization of tapered optical fibre humidity sensors by means of tuning the thickness of nanostructured sensitive coatings", *Sens Actuators B*, vol. 122, no. 2, 2007, pp. 442–449.
- [32] H. Liu, Y. Miao, B. Liu, W. Lin, H. Zhang, B. Song, M. Huang, L. Lin, "Relative Humidity Sensor Based on S-Taper Fibre Coated With SiO₂ Nanoparticles" *IEEE Sens J*, vol. 15, no. 6, 2015, pp. 3424–3428.
- [33] Ramesh H. Bari, Sharad. B. Patil, Anil. R. Bari, "Synthesis, characterization and gas sensing performance of sol-gel prepared nanocrystalline SnO₂ thin films", *International journal on smart sensing and intelligent systems* vol. 7, no. 2, June 2014, pp. 610–629.